

This is a repository copy of *Increasing eigenstructure assignment design degree of freedom using lifting*.

White Rose Research Online URL for this paper:

<https://eprints.whiterose.ac.uk/117411/>

Version: Published Version

---

**Article:**

Chen, Lejun, Pomfret, Andrew James orcid.org/0000-0003-0325-1617 and Clarke, Timothy orcid.org/0000-0002-5238-4769 (2016) Increasing eigenstructure assignment design degree of freedom using lifting. *International Journal of Control*. pp. 1-13. ISSN 0020-7179

<https://doi.org/10.1080/00207179.2016.1236294>

---

**Reuse**

Items deposited in White Rose Research Online are protected by copyright, with all rights reserved unless indicated otherwise. They may be downloaded and/or printed for private study, or other acts as permitted by national copyright laws. The publisher or other rights holders may allow further reproduction and re-use of the full text version. This is indicated by the licence information on the White Rose Research Online record for the item.

**Takedown**

If you consider content in White Rose Research Online to be in breach of UK law, please notify us by emailing [eprints@whiterose.ac.uk](mailto:eprints@whiterose.ac.uk) including the URL of the record and the reason for the withdrawal request.



**Increasing Eigenstructure Assignment Design Degree of Freedom using Lifting**

Journal:	<i>International Journal of Control</i>
Manuscript ID	TCON-2016-0469.R1
Manuscript Type:	Regular Paper
Keywords:	lifting, eigenstructure assignment, causality constraint

SCHOLARONE™  
Manuscripts

To appear in the *International Journal of Control*  
Vol. 00, No. 00, Month 20XX, 1–20

## *Increasing Eigenstructure Assignment Design Degree of Freedom using Lifting*

(Received 00 Month 20XX; accepted 00 Month 20XX)

This paper presents the exposition of an output-lifting eigenstructure assignment (EA) design framework, wherein the available EA design degrees of freedom (DoF) is significantly increased, and the desired eigenstructure of a single-rate full state feedback solution can be achieved within an output feedback system. A structural mapping is introduced to release the output-lifting causality constraint. Additionally, the available design DoF can be further enlarged via involving the input-lifting into the output-lifting EA framework. The newly induced design DoF can be utilised to calculate a structurally-constrained, causal gain matrix which will maintain the same assignment capability. In this paper, the robustification of the output-lifting EA is also proposed, which allows a trade-off between performance and robustness in the presence of structured model uncertainties to be established. A lateral flight control benchmark in the EA literature and a numerical example are used to demonstrate the effectiveness of the design framework.

**Keywords:** lifting; eigenstructure assignment; causality constraint

### 1. Introduction

Eigenstructure assignment (EA) is a mature technique for the design of control systems, especially for flight control system (Alireza & Batool, 2012; B. Chen & Nagarajaiah, 2007; Clake, Ensor, & Griffin, 2003; Farineau, 1989; Kshatriya, Annakkage, Hughes, & Gole, 2007; G. P. Liu & Patton, 1998; Y. Liu, Tan, Wang, & Wang, 2013; Moore, 1976; Ouyang, Richiedei, Trevisani, & Zanardo, 2012; Piou & Sobel, 1994, 1995; Pomfret & Clarke, 2009; Shi & Patton, 2012; Wahrburg & Adamy, 2013; White, 1995; White, Bruyere, & Tsourdos, 2007). EA facilitates control system design by synthesizing a feedback gain matrix that exactly places the closed loop eigenvalues whilst matching the closed loop eigenvectors as closely as possible to a desired set. Some useful properties EA imbues on a system are: stability of response, appropriateness of transient response, decoupling of state or output response and disturbance rejection. Compared with many other competitive approaches exist to manipulate the eigenvalues of the closed-loop system and do not takes into account the role of the eigenvector, EA clearly exploits how system inputs affect mode dynamics and how these mode dynamics will be assigned to system states. Through defining a set of ideal closed-loop eigenstructure (e.g. eigenstructure which represents the realistic handling qualities of the flight control system), the realistic control effect will be guaranteed. In addition, the algorithm itself and the expression of the available design DoF can be highly visible. However, due to the lack of design DoF, e.g. the Kimura condition is not satisfied (Kimura, 1975), output feedback EA usually cannot fully assign the desired eigenstructure. This is an open problem which has been widely discussed in the literature (Andry, Shapiro, & Chung, 1983; L. Chen & Clarke, 2009; Clarke & Griffin, 2004; Pomfret, Clarke, & Ensor, 2005; Roppenecker & O'Reilly, 1989; Srinathkumar, 1978; Zhao & Lam, 2016a, 2016b).

Multirate control systems are those samplers and hold mechanisms that operate at more than one rate. Analysis and design methods for multirate control can be divided into two perspectives, the inferential control approach and the lifting approach (Tangirala, Li, Patwardhan, Shah, & Chen,

2001) which is the focus of this paper. Lifting rearranges various input or output signals, working at different rates of a multirate system, using a uniform, slower frame rate, effectively increasing the number of system inputs and outputs.

This work introduces a formulation for output-lifted EA and first provides the solutions to deal with output-lifting causality constraints that naturally arise. The primary motivation for lifting is to significantly increase the available EA design DoF such that the desired eigenstructure only achievable through single-rate full state feedback solution can be achieved using an output feedback system. The combination of the output-lifting framework and EA effectively solve the open problem in EA literature wherein design DoF is not enough for assigning eigenstructure.

By invoking the Gronwall Lemma, design DoF afforded by output-lifting framework are utilized to derive a time-domain stability robustness measure of output-lifted system in the presence of uncertainty. The Gronwall Lemma was adopted in B. S. Chen and Wong (1987) and Sobel, Banda, and Yeh (1989b) to deduce a time domain robustness measures taking into account of structured and unstructured uncertainties, respectively. The results were extended to discrete system in Sobel, Banda, and Yeh (1989a) and the conservatism of the measure was reduced through using Perron weighting. This paper extends the results from Sobel et al. (1989a); Yu, Piou, and Sobel (1993) and allows the location and the sensitivity of individual eigenvalues can be operated on rather than the spectrum of the all of the system eigenvalues. This further improves the design conservatism. Due to extra DOF offered by output-lifting, a multi-objective optimisation is deduced by taking into account of the trade-off between system stability robustness and mitigation of degradation in equivalent full state feedback performance.

Output-lifting will necessitate a causality constraint which requires structural changes to the gain matrix, a structure mapping is proposed, wherein a directly-calculated, non-causal gain matrix can be utilized to generate a new closed-loop system structure that alleviates the causality constraint. In addition, the available design DoF can be further enlarged by adding input-lifting to the output-lifting EA framework. The newly introduced design DoF can be utilised to calculate a structurally-constrained, causal gain matrix which will maintain the same assignment capability.

The paper is organized as follows. In Sections 2, EA and lifting are briefly introduced. Section 3 proposes output-lifting EA. A less conservative time-domain robustness measurement is developed in Section 4 to ensure the robustification of output-lifting EA. In Section 5, a structure mapping is introduced to alleviate the causality constraint induced by output-lifting. The proposed approaches are demonstrated using a well-known example taken from EA literature and the simulation results are shown in Section 6. By using extra DoF that input-lifting can benefit, a structurally-constrained, causal, lifted controller can be found directly in Section 7 and the associated numerical example is given in Section 8. Concluding remarks are given in Section 9.

## 2. Preliminary

Consider a continuous-time, controllable and observable linear time-invariant system, given by

$$\begin{aligned} \dot{x} &= A_c x + B_c u \\ y &= C_c x \end{aligned} \quad (1)$$

where  $A_c \in \mathbb{R}^{n \times n}$ ,  $B_c \in \mathbb{R}^{n \times r}$ ,  $C_c \in \mathbb{R}^{m \times n}$  and  $D_c \in \mathbb{R}^{m \times r}$ .

Consider a multirate control system, wherein the hold circuit and the sampler work with sample periods of  $q_i T_b$  and  $p_o T_b$  respectively.  $T_b$  is the base sampling period of the system, which can be any common factor of the input and output sampling periods. The main sampling period of the system is given by  $T = l.c.m(p_o, q_i) * T_b$ , *l.c.m* stands for least common multiple. According to the framework for lifting summarized in T. Chen and Francis (1995), the system inputs and outputs

are lifted by  $q$  and  $p$ , respectively, where

$$q = \frac{l.c.m(p_0, q_i)}{q_i} \quad p = \frac{l.c.m(p_0, q_i)}{p_i} \quad (2)$$

The resulting state space lifted system is expressed as

$$\begin{aligned} x(k+1) &= A_L x(k) + B_L \bar{u}(k) \\ \bar{y}(k) &= C_L x(k) + D_L \bar{u}(k) \end{aligned} \quad (3)$$

where  $x(k) := x(kT)$ , and the lifted inputs and outputs are given by

$$\bar{u}(k) = \begin{bmatrix} u(kT) \\ u(kT + pT_b) \\ u(kT + 2pT_b) \\ \vdots \\ u(kT + (pq - p)T_b) \end{bmatrix} \quad \bar{y}(k) = \begin{bmatrix} y(kT) \\ y(kT + qT_b) \\ y(kT + 2qT_b) \\ \vdots \\ y(kT + (pq - q)T_b) \end{bmatrix}$$

In (3), matrices  $A_L \in \mathbb{R}^{n \times n}$ ,  $B_L \in \mathbb{R}^{n \times qr}$ ,  $C_L \in \mathbb{R}^{pm \times n}$  and  $D_L \in \mathbb{R}^{pm \times qr}$  are

$$\left[ \begin{array}{c|c} A_L & B_L \\ \hline C_L & D_L \end{array} \right] = \begin{bmatrix} A^{pq} & \sum_{i=pq-p}^{pq-1} A^i B & \sum_{i=pq-2p}^{pq-p-1} A^i B & \cdots & \sum_{i=0}^{p-1} A^i B \\ C & D_{0,0} & D_{0,1} & \cdots & D_{0,q-1} \\ CA^q & D_{1,0} & D_{1,1} & \cdots & D_{1,q-1} \\ CA^{2q} & D_{2,0} & D_{2,1} & \cdots & D_{2,q-1} \\ \vdots & \vdots & \vdots & \ddots & \vdots \\ CA^{pq-q} & D_{p-1,0} & D_{p-1,1} & \cdots & D_{p-1,q-1} \end{bmatrix}$$

where  $A$ ,  $B$ ,  $C$  and  $D$  are deduced via a discretization of system (1) and the element  $D(i, j)$  is given by

$$D_{i,j} = D\mathcal{X}_{[jp, (j+1)p)}(iq) + \sum_{h=jp}^{(j+1)p-1} CA^{in-1-h} B\mathcal{X}_{[0, iq)}(h) \quad (4)$$

where the characteristic function on integers,  $\mathcal{X}_{[a,b)}(h)$ , conditionally nulls elements within the matrix  $D_L$ ,

$$\mathcal{X}_{[a,b)}(h) = \begin{cases} I & a \leq h < b \\ 0 & \text{otherwise} \end{cases}$$

Obviously, lifting will enlarge the number of system inputs and outputs ( $r \rightarrow qr$  and  $m \rightarrow pm$ ): the design DoF is enlarged. The extra free elements can be parameterised to more closely achieve specified design requirements.

### 3. Output-lifted Eigenstructure Assignment

The output-lifting framework will transform a strictly-proper controllable and observable continuous-time system of (1) into the semi-proper controllable and observable discrete-time sys-

tem of (3), wherein  $D_L$  is non-null (pathological conditions of choosing base sampling frequency and desired eigenvalues to prevent controllability and observability of (3) are described in T. Chen and Francis (1995) and Sheng, Chen, and Shah (2002)).

Assume the system outputs are lifted by a factor  $p$  and the matrix  $C_L$  satisfies  $\text{row}(C_L) = pm \geq \text{rank}(C_L) = n$ , where  $\text{row}(C_L)$  represents the number of rows of  $C_L$ , a static control law  $\bar{u}(k) = K\bar{y}(k) + \bar{r}(k)$  is applied to the lifted system to yield

$$\begin{aligned} x(k+1) &= (A_L + B_L N C_L)x(k) + (B_L + B_L N D_L)\bar{r}(k) \\ \bar{y}(k) &= (C_L + D_L N C_L)x(k) + (D_L + D_L N D_L)\bar{r}(k) \end{aligned}$$

where  $\bar{r}$  is the lifted exogenous input and

$$N = (I - K D_L)^{-1} K \quad (5)$$

**Remark 3.1:** In (5), this time, the term  $I - K D_L$  in  $N$  is assumed to be nonsingular. The constraint is not a curiosity of the exposition presented here. Rather, it represents a system singularity. The feedforward matrix and the feedback matrix form direct forward and backward transmission paths, coupling the input and output through a pair of simultaneous equations. When the constraint is not satisfied, no instantaneous solution exists to these equations for  $\bar{y}$  given  $\bar{r}$  and  $x$ . Thus the constraint is somewhat pathological; it is reasonable to assume that a control system design approach based on meeting performance goals would never give rise to such a situation. Nevertheless, ensuring that this is the case is a simple matter in most cases. This issue will be discussed later in the analysis of the algorithm.

Using the fact that the distinct eigenvalue/eigenvector pair of the closed-loop lifted system,  $\lambda_i$  and  $v_i$ , satisfy

$$(A_L + B_L N C_L)v_i = \lambda_i v_i \quad (6)$$

$$0 = [A_L - \lambda_i I \quad B_L] \begin{bmatrix} v_i \\ N C_L v_i \end{bmatrix} \quad (7)$$

$\begin{bmatrix} v_i \\ N C_L v_i \end{bmatrix}$  thus belongs to the nullspace of  $[A_L - \lambda_i I \quad B_L]$ .

For some  $f_i \in \mathbb{C}^{qr \times 1}$ ,

$$\begin{bmatrix} v_i \\ N C_L v_i \end{bmatrix} = \begin{bmatrix} P_i \\ Q_i \end{bmatrix} f_i \quad (8)$$

where

$$\text{range} \left( \begin{bmatrix} P_i \\ Q_i \end{bmatrix} \right) = \text{null}([A_L - \lambda_i I \quad B_L]) \quad (9)$$

and  $P_i \in \mathbb{C}^{n \times qr}$  is an orthonormal basis for the allowable subspace used to select  $v_i$ . Once the design vector,  $f_i$  has been established, the matrices  $V, S$  can be calculated through

$$V = [v_1 \dots v_l] = [P_1 f_1 \dots P_l f_l] \quad (10)$$

$$S = N C_L V = [Q_1 f_1 \dots Q_l f_l] \quad (11)$$

Substituting (5) into (11) to obtain

$$S = (I - KD_L)^{-1}KC_LV = K(D_LS - C_LV) \quad (12)$$

The gain matrix may be recovered by finding

$$K = S(C_LV + D_LS)^\dagger + Z(I - (C_LV + D_LS))(I - (C_LV + D_LS)^\dagger) \quad (13)$$

where,  $(\cdot)^\dagger$  is the Moore-Penrose inverse operation and  $Z$  is the free matrix to be parameterised.  $l$  represents the  $l$ th assigned eigenvector and associated eigenvalue. Clearly, (13) holds only if  $l \leq pm$ . Consequently for an original un-lifted output feedback system ( $p=1$ ), a maximum of  $m$  poles can be assigned and the other  $(n - m)$  remain unassigned and may become unstable due to the lack of design DOF to parameterise the allowed right eigenvector subspace. For output lifting system, suppose  $pm \geq n$ , (13) holds and the desired eigenstructure of full state feedback can be assigned.

Following the discussion in Remark 3.1, Theorem 3.1 is proposed here to avoid the pathological condition that the term  $I - KD_L$  becomes singular.

**Theorem 3.1:** *By suitably choosing the set of desired eigenvectors, such that  $I - D_LS(C_LV + D_LS)$  is singular,  $Z$  can be parameterized to ensure the non-singularity of  $I - KD_L$ .*

Proof: Suppose  $x \in \ker(C_LV + D_LS)$  and  $Q = S(C_LV + D_LS)^\dagger + Z$ , it is easy to choose a free parameter  $Z$ , such that  $I - D_LQ$  is nonsingular - i.e. there must not exist a zero-valued eigenvalue for  $I - D_LQ$ . That is,  $D_LQ$  must have no eigenvalues of unit value. So

$$D_LQx \neq x \quad (14)$$

$$D_L(S(C_LV + D_LS)^\dagger + Z)x \neq x \quad (15)$$

For any  $x \in \ker(C_LV + D_LS)$ ,

$$Zx = Z(I - (C_LV + D_LS)(C_LV + D_LS)^\dagger)x \quad (16)$$

then (15) can be written as

$$(I - D_LS(C_LV + D_LS)^\dagger - D_LZ(I - (C_LV + D_LS)(C_LV + D_LS)^\dagger))x \neq 0 \quad (17)$$

Using the expression of  $K$  in (13), (17) can be written as

$$(I - D_LK)x \neq 0 \quad (18)$$

Suppose  $y \in \text{range}(C_LV + D_LS)$ , it follows

$$Z(I - (C_LV + D_LS)(C_LV + D_LS)^\dagger)y = 0 \quad (19)$$

By suitably choosing a set of desired eigenvectors, such that  $I - D_LS(C_LV + D_LS)$  is nonsingular:

$$(I - D_LS(C_LV + D_LS))y \neq 0 \quad (20)$$

Substituting (19) to (20) to yield

$$(I - D_L S(C_L V + D_L S))^\dagger - D_L Z(I - (C_L V + D_L S)(C_L V + D_L S)^\dagger))y \neq 0 \quad (21)$$

that is  $(I - D_L K)y \neq 0$ .

The range and kernel describe a complete space,

$$\mathbb{R}^n = \text{range}(C_L V + D_L S) \oplus \text{ker}(C_L V + D_L S) \quad (22)$$

For any vector  $z$  in full space, where  $\{z\} = \{x\} \cup \{y\}$

$$(I - D_L K)z \neq 0 \quad (23)$$

Since the non-singularity of  $I - D_L K$  is necessary and sufficient to ensure the non-singularity of  $I - K D_L$  (Fletcher, 1981),  $Z$  can be chosen to ensure the term  $I - K D_L$  to be nonsingular. ■

The gain matrix can be recovered since  $\text{rank}(C_L) = n \leq \text{row}(C_L)$ . Using this  $K$ , the equivalent of state feedback EA can be achieved since the allowable subspaces of output-lifting feedback and state feedback corresponding to each desired eigenvalue are same, the proof of which is in Theorem 3.2 below.

**Theorem 3.2:** *Suppose  $A_s, B_s$  is a discrete-time system working at the main sampling period, the allowable subspace of the output-lifted system is the same as for the single main sampling rate system.*

$$\text{null}([A_L - \lambda_i I, B_L]) = \text{null}([A_s - \lambda_i I, B_s]) \quad (24)$$

Proof: Let  $A_c, B_c, C_c, D_c$  and  $A, B, C, D$  represent a continuous-time system and an equivalent system sampled at a base sampling period,  $T_b$ .  $A$  and  $B$  can be given by

$$A = e^{T_b A_c} \quad B = \int_0^{T_b} e^{\tau A_c} d\tau B_c \quad (25)$$

Suppose system outputs are lifted by a ratio  $p$ , the main sampling period becomes  $pT_b$ , and

$$A_s = e^{pT_b A_c} = A^p \quad (26)$$

$$B_s = \int_0^{pT_b} e^{\tau A_c} d\tau B_c = \sum_{i=1}^p \int_{(i-1)T_b}^{iT_b} e^{\tau A_c} d\tau B_c \quad (27)$$

Using the integral identity

$$\int_{\alpha}^{\beta} f(x) dx = \frac{\beta - \alpha}{\psi - \varphi} \int_{\varphi}^{\psi} f\left(\frac{\beta - \alpha}{\psi - \varphi} \tau + \frac{\beta\psi - \alpha\varphi}{\psi - \varphi}\right) d\tau \quad (28)$$



Equation (27) can be written as

$$\begin{aligned}
 B_s &= \sum_{i=1}^p \int_{(i-1)T_b}^{iT_b} e^{\tau A_c} d\tau B_c \\
 &= \int_0^{T_b} e^{\tau A_c} d\tau B_c + \sum_{i=2}^p \int_{(i-1)T_b}^{iT_b} e^{\tau A_c} d\tau B_c \tag{29}
 \end{aligned}$$

$$= \int_0^{T_b} e^{\tau A_c} d\tau B_c + \sum_{i=1}^{p-1} \int_{(i-1)T_b}^{iT_b} e^{(\tau+iT_b)A_c} d\tau B_c \tag{30}$$

$$= \int_0^{T_b} e^{\tau A_c} d\tau B_c + \sum_{i=1}^{p-1} e^{iT_b A_c} \int_0^{T_b} e^{\tau A_c} d\tau B_c \tag{31}$$

$$= \sum_{i=0}^{p-1} (A^i)B = B_L \tag{32}$$

Therefore, by inspection, (24) is true. ■

#### 4. Robustification

In this section, the design DoF generated by output-lifting framework is utilized in a post assignment process, to achieve the robustification of the output-lifting EA. A multi-objective optimisation is established to improve the stability robustness, whilst to mitigate the degradation in equivalent full state feedback performance.

##### 4.1 Robustness measure with time-varying uncertainty

Suppose the lifted system is subject to time-varying parametric structured uncertainty  $\Delta A_L(k), \Delta B_L(k), \Delta C_L(k)$  and  $\Delta D_L(k)$ , satisfy  $\Delta A_L^+(k) \leq A_m, \Delta B_L^+(k) \leq B_m, \Delta C_L^+(k) \leq C_m$ , and  $\Delta D_L^+(k) \leq D_m$ . In this paper,  $(\cdot)^+$  replaces the entries of matrix by their absolute values and  $(\cdot)_m$  represents the absolute value of the maximum variation of time varying uncertainties, on an element by element basis. A stability robustness measure for an output-lifted system is defined in Theorem 4.1.

**Theorem 4.1:** *The uncertain closed-loop system is asymptotically stable for all  $\Delta A_L(k), \Delta B_L(k), \Delta C_L(k)$  and  $\Delta D_L(k)$  if*

$$\sum_{i=1}^n \frac{(w_i)^+(A_{cm} + E_m \Xi)(v_i)^+}{1 - |\lambda_i|} < 1 \tag{33}$$

where

$$\begin{aligned}
 A_{cm} &= A_m + B_m(NC_L)^+ + (B_L N)^+ C_m + B_m N^+ C_m \\
 E_m &= (B_L N)^+ D_m + B_m N^+ C_m \tag{34}
 \end{aligned}$$

$$\Xi = (I - N^+ D_m)^{-1} (N^+ (C_L^+ + C_m)) \tag{35}$$

and  $V$  and  $\lambda_i$  are the modal matrix and the  $i$ th eigenvalues of  $(A_L + B_L N C_L)$  respectively.  $w_i$  and  $v_i$  are achieved left and right eigenvectors associated with  $\lambda_i$ .

1  
2  
3 Proof: See Appendix A. ■

4 **Remark 4.1:** Note that minimization of the left side of (33) will increase the stability robustness  
5 of the system. A large denominator in (33) indicates that the eigenvalue is far away from the unit  
6 circle, which exhibits greater stability robustness. Also, choosing different eigenvectors directions  
7 to decrease the numerator of (33) can be considered as reducing the sensitivity of the closed-loop  
8 system to the given structured perturbation.  
9

10 From the left side of (33), the stability robustness of the  $i$ th eigenvalue/eigenvector pair can be  
11 measured by using (36).  
12

$$13 \quad J_{si} = \min_{f_i, \lambda_i} \frac{(w_i)^+ (A_{cm} + E_m \Xi)(v_i)^+}{1 - |\lambda_i|} \quad (36)$$

#### 14 15 16 17 18 **4.2 Multi-objective output-lifting EA**

19 Criteria associated with retaining full state feedback performance is also considered alongside  
20 robustification. In this paper, the performance measure is proposed to minimise the errors between  
21 the desired and the achieved eigenstructure. A cost function as shown in (37) is used to fulfil the  
22 task.  
23  
24

$$25 \quad J_{vi} = \min_{f_i, \lambda_i} \|v_{id} - P_i f_i\|_2^2 \quad (37)$$

$$26 \quad \text{s.t. } |\lambda_{id} - \lambda_{ia}| < r$$

27 where  $f_i$  and  $v_{id}$  represent the  $i$ th design vector and the  $i$ th desired right eigenvector.  $\|\cdot\|$  denotes  
28 the vector or matrix 2-norm.  $\lambda_{id}$  and  $\lambda_{ia}$  represent the desired and achieved eigenvalue, respectively.  
29  $P_i$  is the allowable subspace for the  $i$ th achieved eigenvalue.  $r$  is the radius of the allowed region  
30 for the  $i$ th eigenvalue.  
31  
32

33 In improving the stability robustness, whilst, mitigating the performance degradation, a multi-  
34 objective optimisation is given by  
35  
36

$$37 \quad J_i = a_i J_{si} + b_i J_{vi} \quad (38)$$

38 where,  $J_{si}$ , defined in (36), represents the stability robustness measure. The weighting parameters  
39  $a_i$  and  $b_i$  control the relative significance of the robustness and the performance terms of the  $i$ th  
40 eigenvalue/eigenvector pair.  
41  
42  
43  
44

### 45 **5. Releasing causality constraints using structure mapping**

46 Since the outputs of the controller at current time only depend on the output of the plant at or  
47 before current time, lifting system outputs will introduces causality constraints upon the constant  
48 gain matrix. For example, suppose lifting system inputs and outputs as defined in (4), the resulting  
49 feedback gain matrix  $K$  must be lower triangular, under causality. With the causality constraint  
50 enforced, any *fully-populated* gain matrix, calculated as a general outcome of the direct use of EA  
51 on an output-lifted system is non-causal and even unstable.  
52  
53

54 In this section, a structure mapping is proposed to release the causality constraint, whilst allowing  
55 the non-causal full gain matrix to be utilised. The structure mapping is achieved through the change  
56 of implementation structure of the closed-loop system, which is shown in Figs. 1 and 2.  
57  
58  
59  
60

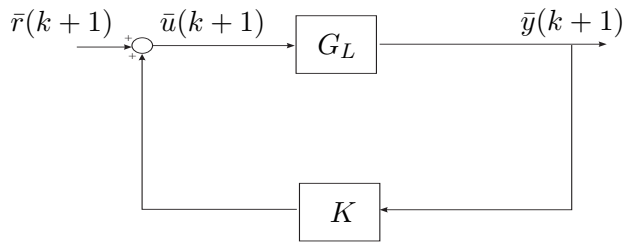


Figure 1. Closed-loop structure under causality constraint

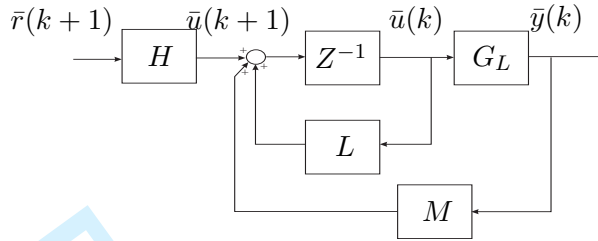


Figure 2. Closed-loop structure without causality constraint

In Fig. 1, the direct-calculated non-causal gain matrix  $K$  satisfies

$$\begin{aligned} \bar{u}(k+1) &= K\bar{y}(k+1) + \bar{r}(k+1) \\ &= K[C_L\bar{x}(k+1) + D_L\bar{u}(k+1)] + \bar{r}(k+1) \\ &= NC_L(A_L\bar{x}(k) + B_L\bar{u}(k)) + (I - KD_L)^{-1}\bar{r}(k+1) \end{aligned} \quad (39)$$

where the term  $I - KD$  is assumed to be nonsingular (the implications of this restriction is discussed earlier). In Fig. 2, the new implementation structure releases the causality constraint. Appropriate equations can be obtained directly from the figure.

$$\begin{aligned} \bar{u}(k+1) &= L\bar{u}(k) + M\bar{y}(k) + H\bar{r}(k+1) \\ &= L\bar{u}(k) + MD_L\bar{u}(k) + MC_L\bar{x}(k) + H\bar{r}(k+1) \end{aligned} \quad (40)$$

A mapping between (39) and (40) are given by

$$MC_L = NC_LA_L \quad (41)$$

$$L + MD_L = NC_LB_L \quad (42)$$

$$H = (I - KD_L)^{-1} \quad (43)$$

Using above structural mapping, matrices  $M$ ,  $L$  and  $H$  can be calculated based on non-casual matrix  $K$ . The causality constraint is released and the eigenstructure of the closed-loop system in Fig. 1 can be maintained.

Table 1. Achieved Eigenstructure (Full state feedback case)

Roll mode	Dutch roll mode	Flight-path mode
$0.0002 \pm 0.0001i$	$0.3188 \pm 0.3185i$	0.7072
$-0.2226 \mp 0.1480i$	$0.0000 \pm 0.0001i$	0.0001
0.9636	$-0.0000 \mp 0.0000i$	0.0001
$-0.0000 \mp 0.0001i$	0.8819	-0.0002
$0.0001 \pm 0.0002i$	$0.0978 \pm 0.0980i$	0.7070
$0.8841 \pm 0.0709i$	$0.9202 \pm 0.0738i$	0.9802

## 6. Example 1

A fifth-order FPCC Lateral Dynamics Flight Control benchmark within the EA literature (Sobel & Lallman, 1989) is illustrated here. The continuous-time state space system is given by

$$A_c = \begin{bmatrix} -0.340 & 0.0517 & 0.001 & -0.997 & 0 \\ 0 & 0 & 1 & 0 & 0 \\ -2.69 & 0 & -1.15 & 0.738 & 0 \\ 5.91 & 0 & 0.138 & -0.506 & 0 \\ -0.340 & 0.0517 & 0.001 & -0.0031 & 0 \end{bmatrix} \quad (44)$$

$$B_c = \begin{bmatrix} 0.0755 & 0 & 0.0246 \\ 0 & 0 & 0 \\ 4.48 & 5.22 & -0.742 \\ -5.03 & 0.0998 & 0.984 \\ 0.0755 & 0 & 0.0246 \end{bmatrix} \quad C_c = \begin{bmatrix} 0 & 1 & 0 & 0 & 0 \\ 0 & 0 & 0 & 1 & 0 \\ 0 & 0 & 0 & 0 & 1 \end{bmatrix} \quad (45)$$

The states  $[\beta \ \phi \ p \ r \ \gamma]'$  correspond to sideslip angle, bank angle, roll rate, yaw rate and flight path angle, respectively. The control inputs  $[\delta_r \ \delta_a \ \delta_c]'$  denote the surface deflections of the rudder, ailerons and vertical canard respectively. The desired eigenvalues, corresponding to Dutch roll, Roll and Flight path modes are  $\lambda_{dr}^d = -2 \pm j2$ ,  $\lambda_{roll}^d = -3 \pm j2$  and  $\lambda_s^d = -0.5$ , respectively. The design goal is a yaw pointing/lateral translation control law in which the lateral/directional flight-path response is decoupled from the yaw rate response. Also, both of these responses should be decoupled from the roll rate and bank angle response. Hence, the desired eigenvectors are chosen as:

$$\begin{aligned} v_{dr}^d &= [0 \ 0 \ 0 \ 1 \ 0]^T \pm j [1 \ 0 \ 0 \ 1 \ 0]^T \\ v_{roll}^d &= [0 \ 0 \ 1 \ 0 \ 0]^T \pm j [0 \ 1 \ 1 \ 0 \ 0]^T \\ v_s^d &= [1 \ 0 \ 0 \ 0 \ 1]^T \end{aligned} \quad (46)$$

Suppose the holder and the sampler works at the main sampling period  $0.04sec$  and the base sampling period  $0.01sec$ , respectively. The system outputs are chosen to be lifted by 4. After discretisation at the main sampling period, the desired eigenvalues for the roll, Dutch roll and flight-path modes become  $0.8804 \pm 0.0709i$ ,  $0.9202 \pm 0.0738i$ ,  $0.9802$  in the unit circle.

Full state feedback EA and output-lifted EA are both implemented on benchmark. Results are presented to demonstrate the equivalence of performance. In tables 1 and 2, top and bottom rows show the achieved eigenvectors and eigenvalues, respectively. Clearly, output-lifting EA can achieve the same eigenstructure as achieved using full state feedback. Figs. 5 and 6 show the nominal

Table 2. Achieved Eigenstructure (Output-lifted feedback case)

Roll mode	Dutch roll mode	Flight-path mode
$0.0002 \pm 0.0001i$	$0.3188 \pm 0.3185i$	0.7072
$-0.2226 \mp 0.1480i$	$0.0000 \pm 0.0001i$	0.0001
0.9636	$-0.0000 \mp 0.0000i$	0.0001
$-0.0000 \mp 0.0001i$	0.8819	-0.0002
$0.0001 \pm 0.0002i$	$0.0978 \pm 0.0980i$	0.7070
$0.8841 \pm 0.0709i$	$0.9202 \pm 0.0738i$	0.9802

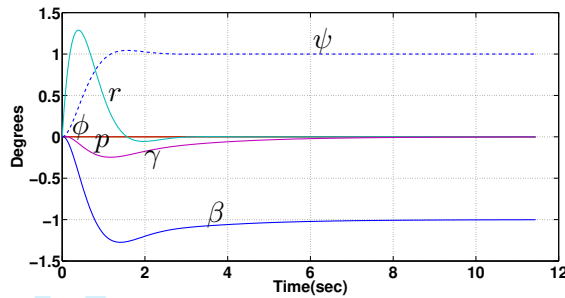


Figure 3. Full State Feedback Responses to a Unit Heading Command

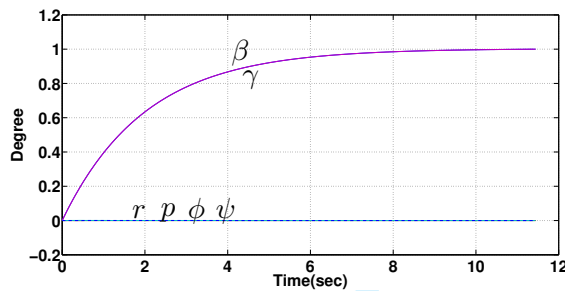


Figure 4. Full State Feedback Responses to a Flight-Path Command

outputs responses of output-lifted system to unit heading and flight-path commands respectively, wherein, the nominal mode decoupling information is shown, which is same as that of a full state feedback design as shown in Figs. 3 and 4, representing the best possible performance.

Continuous-time structured uncertainty is assumed, in line with the literature, to be of the form

$$\Delta A_c = \begin{bmatrix} 0.1 & 0 & 0 & 0 & 0 \\ 0 & 0 & 0 & 0 & 0 \\ 0 & 0.1 & 0 & 0 & 0 \\ 0 & 0 & 0.1 & 0 & 0 \\ 0 & 0 & 0 & 0.1 & 0 \end{bmatrix}, \Delta B_c = 0 \tag{47}$$

The allowed migration regions for the real and imaginary parts of the eigenvalues of the dutch roll, roll and flight-path modes are 0.03, 0.03, and 0.01 respectively.

The solution of nominal output-lifted system offers relatively poor robustness since the value of left hand side of (33) equates to 1.4769. In view of increasing the stability robustness of the system, two robust solutions of the gain matrices are given. In calculating one solution, increasing stability

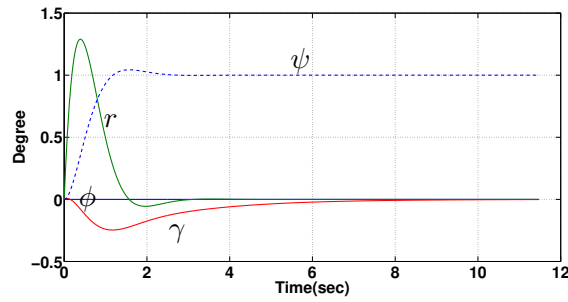


Figure 5. Lifted Output Responses to a Unit Heading Command

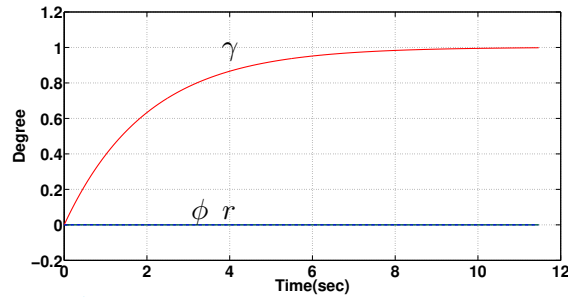


Figure 6. Lifted Output Responses to a Flight-Path Command

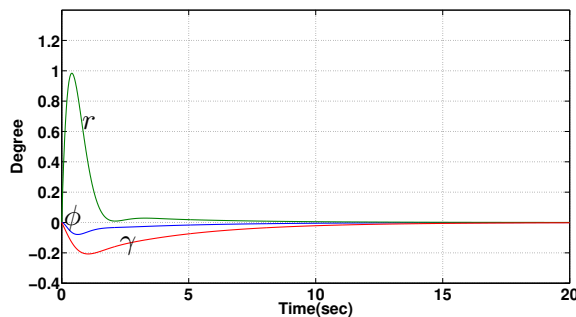


Figure 7. Lifted Output Responses to a Unit Heading Command after robustification without performance protection

robustness without performance protection is considered, that is, in (38),  $a_i = 10, b_i = 0$  ( $i = 1, \dots, n$ ). This solution yields a value of 0.3845 for the left hand side of (38), which demonstrates better robustness.

Another solution is calculated, combining the performance protection. In this case,  $a_i, b_i = 1$  ( $i = 1, \dots, n$ ) in (38), a value of 0.9487 is yielded for the left hand side of (33). Compared with the value calculated under the circumstances not involving performance protection, the robustness is reduced and the performance is improved.

The following time histories demonstrate the results of the robustification.

Fig. 7 and Fig. 8 depict output responses to unit heading and flight-path commands without performance protection. Output responses to unit heading and flight-path commands with performance protection is shown in Figs. 9 and 10. These figures show that performance protection has done a lot to preserve the decoupling action of the controller although, as expected, responses have suffered some degradation due to robustification.

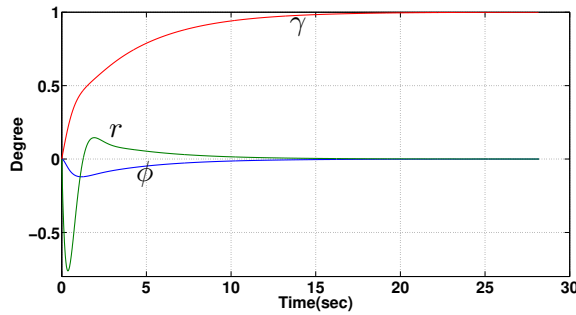


Figure 8. Lifted Output Responses to a Flight-Path Command after robustification without performance protection

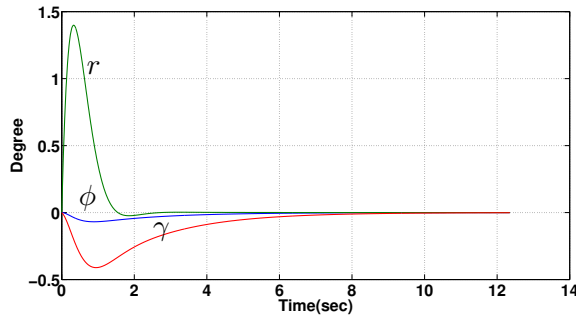


Figure 9. Lifted Output Responses to a Unit Heading Command after robustification with performance protection

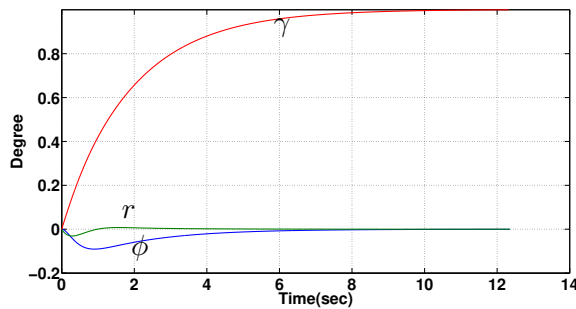


Figure 10. Lifted Output Responses to a Flight-Path Command after robustification with performance protection

### 7. Input-lifting benefits

Lifting system inputs can increase the dimension of the allowable subspace  $\left( [ P_i^T \ Q_i^T ]^T \right)$  so that each desired eigenvector can be exactly achieved (i.e. all of the elements in each) (Patton, Liu, & Patel, 1995). Lifting system *outputs* can be used to enable assignment of all of the desired eigenvectors. Therefore, if system inputs and outputs are *both* lifted (dual-lifting), all of the desired eigenvectors can be exactly achieved. As an additional bonus, since the size of the gain matrix is increased considerably after the dual-lifting process, many elements in the gain matrix are still available, as further design freedom, and can be parameterised.

As mentioned in the last section, lifting system outputs induces a causality constraint such that, either a structural mapping must be invoked, or some elements in the gain matrix must be nulled, resulting in a directly-causal gain matrix of appropriate form. It is possible to parameterise and

exploit some of the extra DoF, described above, to impose this structure. So, if the available DoF are larger or equal to the sum of the DoF used for assigning eigenstructure *and* satisfying the causality constraint, then a solution for the EA gain matrix which simultaneously satisfies the causality constraint can be found directly. The procedure for this is now presented.

**Proposition 7.1:** *For the dual-lifting case, wherein subsets of samplers or hold circuits works at different rates, the distribution of the DoF for finding a directly-causal gain matrix is given by*

$$\sum_{i=1}^r q_i n + t \leq \sum_{i=1}^r \sum_{j=1}^m q_i p_j \quad (48)$$

$$t = \sum_{i=1}^r \sum_{j=1}^m q_i p_j - \left( rm + \sum_{i=1}^r \sum_{k=1}^{q_i-1} \sum_{j=1}^m \left\{ \text{round}\left(\frac{k p_j}{q_i} + 1\right) \right\} \right) \quad (49)$$

where  $t$  equates the number of the fixed null elements inside the gain matrix constrained by causality.  $q_i$  and  $p_i$  are lifting ratios of the  $i$ th input and output respectively.

After choosing suitable dual-lifting ratios to satisfy Proposition 1, the free parameter matrix  $Z$  in (13) can be used to formulate a causal gain matrix. This process for finding a suitable  $Z$  matrix can be achieved by using a permutation matrix  $U_{\delta \times mprq}$  (Pomfret, 2006),  $\delta$  is the number of the null elements of the gain matrix caused by the causality constraint. In each row of  $U$ , only one element is unity, others are all null, which can be used to select the specified elements of the vector version of the gain matrix. Therefore, all null elements in the gain matrix are selected by using  $U$ , which is given by

$$U \text{vec}(K) = 0 \quad (50)$$

where  $\text{vec}(\cdot)$  denotes column-wise vectorisation of a matrix. Substituting (13) into (50) yields

$$U \text{vec}(K) = 0 \quad (51)$$

$$U \text{vec}(K_0 + Z(I - YY^\dagger)) = 0 \quad (52)$$

$$U \text{vec}(K_0) + U \text{vec}(Z(I - YY^\dagger)) = 0 \quad (53)$$

where  $K_0 = S(C_L V + D_L S)^\dagger$  and  $Y = C_L V + D_L S$ .

Applying the identity  $\text{vec}(AYB) = (B^T \otimes A) \text{vec}(Y)$  to (53) yields

$$U \text{vec}(K_0) + U((I - YY^\dagger)^T \otimes I) \text{vec}(Z) = 0 \quad (54)$$

Define  $\Xi = (I - YY^\dagger)^T \otimes I$ , (54) can be written as

$$U \Xi \text{vec}(Z) = -U \text{vec}(K_0) \quad (55)$$

Provided the identity  $U \Xi$  is a full row rank, it follows

$$\text{vec}(Z) = -(U \Xi)^\dagger U \text{vec}(K_0) + (I - (U \Xi)^\dagger U \Xi) \text{vec}(\tilde{Z}) \quad (56)$$

where  $\tilde{Z}$  represents a free matrix. If  $\text{rank}(U \Xi) = \delta$ , and DoF of the lifted system satisfies (48), the free matrix  $Z$  in (13) can be find and the causal matrix  $K$  can be calculated to assign the eigenstructure under the causality constraint.



### 8. Design example 2

To demonstrate direct-causal feedback gain matrix design, consider the following system and its desired eigenstructure (Patton et al., 1995):

$$A = \begin{bmatrix} 0 & 1 & 0 \\ 0 & 0 & 1 \\ -6 & -11 & -6 \end{bmatrix} \quad B = \begin{bmatrix} 1 & 1 \\ 0 & 1 \\ 1 & 1 \end{bmatrix} \quad C = \begin{bmatrix} 1 & 0 & 0 \\ 0 & 1 & 0 \\ 0 & 0 & 1 \end{bmatrix} \quad (57)$$

$$\lambda = \{-0.5, -0.6, -0.7\} \quad V_d = \begin{bmatrix} 1 & 0 & 0 \\ 0 & 1 & 0 \\ 0 & 0 & 1 \end{bmatrix} \quad (58)$$

Let the main sampling period be 0.1sec and the two holds operate at periods of 0.05sec and 0.02sec, respectively. Three samplers are assumed to work at periods of 0.02sec, 0.05sec and 0.1sec, respectively. The lifting ratios of two system inputs are selected to be 2 and 5, respectively, and those of three system outputs are selected to be 5, 2 and 1, respectively. The desired discrete eigenvalues are given by

$$\lambda_{dis} = \{0.9512, 0.9418, 0.9324\} \quad (59)$$

Notice that the causality constraint requires that the structure of the causal gain matrix to satisfy

$$\begin{bmatrix} u_1(0s) \\ u_1(0.05s) \\ u_2(0s) \\ u_2(0.02s) \\ u_2(0.04s) \\ u_2(0.06s) \\ u_2(0.08s) \end{bmatrix} = \begin{bmatrix} \times & 0 & 0 & 0 & 0 & \times & 0 & \times \\ \times & \times & \times & 0 & 0 & \times & \times & \times \\ \times & 0 & 0 & 0 & 0 & \times & 0 & \times \\ \times & \times & 0 & 0 & 0 & \times & 0 & \times \\ \times & \times & \times & 0 & 0 & \times & 0 & \times \\ \times & \times & \times & \times & 0 & \times & \times & \times \\ \times & \times & \times & \times & \times & \times & \times & \times \end{bmatrix} \cdot \begin{bmatrix} y_1(0s) \\ y_1(0.02s) \\ y_1(0.04s) \\ y_1(0.06s) \\ y_1(0.08s) \\ y_2(0s) \\ y_2(0.05s) \\ y_3(0s) \end{bmatrix}$$

where ' $\times$ ' represent the free elements to be parameterized and the zero elements denote the causality constraints.

Recall (48), in this example,  $t = 20$ ,  $\sum_{i=1}^r q_i n = 21$ ,  $\sum_{i=1}^r \sum_{j=1}^m q_i p_j = 56$ . Since the distribution of DoF satisfies (48), the matrix  $Z$  can be calculated using (56).

$$Z = \begin{bmatrix} 1.61 & 1.83 & -3.77 & -4.11 & 1.06 & -6.40 & 0.43 & -2.64 \\ 0.16 & -0.82 & -1.57 & 3.96 & -0.72 & 1.33 & 0.43 & 0.77 \\ 2.24 & 1.87 & -4.59 & -4.98 & 0.98 & -7.89 & -0.01 & -3.48 \\ 0.23 & 2.54 & -2.56 & -2.77 & 0.49 & -3.55 & -0.10 & -1.60 \\ 0.01 & 0.08 & 0.14 & -0.32 & -0.05 & -0.09 & -0.17 & -0.11 \\ 0.19 & 0.15 & 0.13 & 0.12 & -0.66 & -0.03 & -0.06 & -0.04 \\ 0.00 & 0.00 & 0 & 0 & 0 & 0 & 0 & 0 \end{bmatrix}$$

Substituting matrix  $Z$  into (13) to yield a directly-causal gain matrix  $K_c$ , given by

$$K_c = \begin{bmatrix} -7.56 & 0 & 0 & 0 & 0 & -13.41 & 0 & -4.79 \\ 8.22 & 0.59 & -5.22 & 0 & 0 & 7.07 & 0.24 & 4.37 \\ -8.10 & 0 & 0 & 0 & 0 & -15.44 & 0 & -7.46 \\ -5.37 & 1.58 & 0 & 0 & 0 & -7.59 & 0 & -4.04 \\ -0.36 & 0.10 & 0.45 & 0 & 0 & -0.25 & 0 & -0.83 \\ 5.61 & 1.26 & -2.05 & -2.26 & 0 & 4.10 & 0.21 & 1.16 \\ 11.81 & 2.32 & -4.92 & -5.37 & 1.32 & 8.85 & 0.36 & 3.31 \end{bmatrix}$$

and  $Uvec(K_c) = 0$ . Using  $K_c$ , the desired eigenstructure is achieved.

## 9. Conclusions

Through exposing design DoF induced by output-lifting EA, the desired eigenstructure of a single-rate full state feedback solution can be achieved with an output feedback system, and output-lifting causality constraint is released by the structural mapping. In addition, the available design DoF can be further enlarged via involving the input-lifting in the output-lifting EA framework. The newly introduced design DoF can be utilised to calculate a structurally-constrained, causal gain matrix which will maintain the same assignment capability. In addition, a less conservative time-domain robustness measurement is developed to ensure the robustification of output-lifting EA.

## Appendix. A

### Proof of Theorem 4.1

Consider an lifted system with time-varying uncertainty

$$x(k+1) = (A_L + \Delta A_L(k))x(k) + (B_L + \Delta B_L(k))\bar{u}(k) \quad (60)$$

$$\bar{y}(k) = (C_L + \Delta C_L(k))x(k) + (D_L + \Delta D_L(k))\bar{u}(k) \quad (61)$$

$$\bar{u}(k) = K\bar{y}(k) \quad (62)$$

Substituting (61) into (62) yields

$$(I - KD_L)\bar{u}(k) = K(C_L + \Delta C_L(k))x(k) + K\Delta D_L(k)\bar{u}(k) \quad (63)$$

From (63),

$$\bar{u}(k) = N(C_L + \Delta C_L(k))x(k) + N\Delta D_L(k)\bar{u}(k) \quad (64)$$

Now substitute (64) into (60) to obtain

$$x(k+1) = A_{cl}x(k) + \Delta A_{cl}(k)x(k) + \Delta E(k)\bar{u}(k) \quad (65)$$

where

$$\Delta A_{cl}(k) = \Delta A_L(k) + \Delta B_L(k)NC_L + (B + \Delta B_L(k))N\Delta C_L(k) \quad (66)$$

$$A_{cl} = A_L + B_LNC_L \quad (67)$$

$$\Delta E(k) = (B_L + \Delta B_L(k))N\Delta D_L(k) \quad (68)$$

Let  $M$  represent the modal matrix of  $A_L + B_LNC_L$  and define matrix  $D$  as a diagonal matrix with real positive entries, then  $MD$  also represents a modal matrix. Using the modal similarity

transformation, it follows

$$x(k) = D^{-1}M^{-1}\bar{z}(k) \tag{69}$$

Applying the similarity transformation to (65) and the solution of  $\bar{z}(k)$  is given by

$$\begin{aligned} \bar{z}(k) = & D^{-1}\Lambda^k D\bar{z}(0) + \sum_{j=0}^{k+1} \Lambda^{k-j-1} D^{-1} M^{-1} \Delta A_{cl}(j) M D\bar{z}(j) \\ & + \sum_{j=0}^{k+1} \Lambda^{k-j-1} D^{-1} M^{-1} \Delta E(j) \bar{u}(j) \end{aligned} \tag{70}$$

where  $\Lambda$  is a diagonal matrix of the eigenvalues of  $A_c$ . Applying the absolute value operator to get

$$\begin{aligned} \bar{z}^+(k) \leq & D^{-1}\Lambda^k D\bar{z}^+(0) + \sum_{j=0}^{k+1} \Lambda^{k-j-1} D^{-1} (M^{-1})^+ \Delta A_{cl}(j) M^+ D\bar{z}^+(j) \\ & + \sum_{j=0}^{k+1} \Lambda^{k-j-1} D^{-1} (M^{-1})^+ \Delta E(j) \bar{u}^+(j) \end{aligned} \tag{71}$$

Also, (64) can be written as

$$\bar{u}^+(k) = N^+(C_L^+ + C_m)x^+(k) + N^+D_m\bar{u}^+(k) \tag{72}$$

Then

$$\bar{u}^+(k) \leq \Xi M^+ D\bar{z}^+(k) \tag{73}$$

Substituting (73) into (71) yields

$$\begin{aligned} \bar{z}^+(k) \leq & D^{-1}\Lambda^k D\bar{z}^+(0) + \sum_{j=0}^{k+1} \Lambda^{k-j-1} D^{-1} (M^{-1})^+ \Delta A_{cl}(j) M^+ D\bar{z}^+(j) \\ & + \sum_{j=0}^{k+1} \Lambda^{k-j-1} D^{-1} (M^{-1})^+ \Delta E(j) \Xi M^+ D\bar{z}^+(j) \end{aligned} \tag{74}$$

Using the fact that  $\|\Lambda^k\| \leq \alpha^k$  and  $\alpha = \max|\Lambda|$ , it follows

$$\bar{z}^+(k) \leq D^{-1}\alpha^k D\bar{z}^+(0) + \sum_{j=0}^{k+1} \alpha^{k-j-1} D^{-1} (M^{-1})^+ (A_{cm} + E_m \Xi) M^+ D\bar{z}^+(j) \tag{75}$$

Then

$$\bar{z}^+(k)\alpha^{-k} \leq \bar{z}^+(0) + \sum_{j=0}^{k+1} \alpha^{-1} D^{-1} (M^{-1})^+ (A_{cm} + E_m \Xi) M^+ D\alpha^{-j}\bar{z}^+(j) \tag{76}$$

Using the Discrete Gronwall Lemma, (76) can be written as

$$\bar{z}^+(k)\alpha^{-k} \leq \bar{z}^+(0)(1 + \alpha^{-1}(D^{-1}(M^{-1})^+(A_{cm} + E_m\Xi)M^+D))^k \quad (77)$$

Now multiply both sides of (77) by  $\alpha^k$  and then take the norm for both sides of (77) to obtain

$$\|\bar{z}^+(k)\| \leq \|\bar{z}^+(0)\|(\alpha + \|D^{-1}(M^{-1})^+(A_{cm} + E_m\Xi)M^+D\|)^k \quad (78)$$

From (78), a sufficient condition for the asymptotically stable response is given by

$$\|D^{-1}(M^{-1})^+(A_{cm} + E_m\Xi)M^+D\| < 1 - \alpha \quad (79)$$

which equates to

$$\|(M^{-1})^+(A_{cm} + E_m\Xi)M^+\|_{2D} < 1 - \alpha \quad (80)$$

Since the matrix term inside the norm of the above equation only contains the positive elements, the condition in (80) can be written as

$$\inf_D \|(M^{-1})^+(A_{cm} + E_m\Xi)M^+\|_{2D} < 1 - \alpha \quad (81)$$

Using the fact that

$$\inf_D \|A^+\|_{2D} = \rho(A^+) \quad (82)$$

where  $\rho$  represents the perron eigenvalue of the matrix with all positive entries. (81) can be written as

$$\rho[(M^{-1})^+(A_{cm} + E_m\Xi)M^+] < 1 - \alpha \quad (83)$$

Since the eigenvalues of  $AB$  and of  $BA$  are identical for all square  $A$  and  $B$ , (83) equates to

$$\rho[M^+(M^{-1})^+(A_{cm} + E_m\Xi)] < 1 - \alpha \quad (84)$$

Dividing both sides of (84) by  $(1 - \alpha)$  yields

$$\rho\left[\frac{M^+(M^{-1})^+(A_{cm} + E_m\Xi)}{1 - \alpha}\right] < 1 \quad (85)$$

which equates to

$$\rho\left[\frac{\sum_{i=1}^n v_i^+(w_i)^+(A_{cm} + E_m\Xi)}{1 - \alpha}\right] < 1 \quad (86)$$

Using this result, if  $A^+ \leq B^+$ , then

$$\lambda_{max}(A^+) \leq \lambda_{max}(B^+) \quad (87)$$

Substitute (87) into (86) and invoke the property  $|\Lambda^k| \leq \alpha^k$ , a sufficient condition is given by

$$\rho\left[\sum_{i=1}^n \frac{v_i^+(w_i)^+(A_{cm} + E_m \Xi)}{1 - |\lambda_i|}\right] < 1 \quad (88)$$

The spectral radius of the square matrices  $A, B$  satisfies (89), which can be proven by using *Rayleigh's principle*.

$$\rho(A) + \rho(B) \geq \rho(A + B) \quad (89)$$

Applying the above matrix property to (88) to get

$$\sum_{i=1}^n \rho\left[\frac{v_i^+(w_i)^+(A_{cm} + E_m \Xi)}{1 - |\lambda_i|}\right] < 1 \quad (90)$$

which can be simplified by

$$\sum_{i=1}^n \frac{(w_i)^+(A_{cm} + E_m \Xi)v_i^+}{1 - |\lambda_i|} < 1 \quad (91)$$

## References

- Alireza, E. A., & Batool, L. (2012). Application of matrix perturbation theory in robust control of large-scale systems. *Automatica*, 48(8), 1868–1873.
- Andry, A. N., Shapiro, E. Y., & Chung, J. C. (1983). Eigenstructure assignment for linear systems. *IEEE Transactions on Aerospace and Electronic Systems*, 19(5), 711-727.
- Chen, B., & Nagarajaiah, S. (2007). Linear-matrix-inequality-based robust fault detection and isolation using the eigenstructure assignment method. *Journal of Guidance, Control and Dynamics*, 30(6), 1831-1835.
- Chen, B. S., & Wong, S. S. (1987). Robust linear controller design: Time domain approach. *IEEE Transactions on Automatic Control*, 32(2), 161-164.
- Chen, L., & Clarke, T. (2009). *Multirate eigenstructure assignment using lifting*. Unpublished doctoral dissertation, University of York.
- Chen, T., & Francis, B. (1995). *Optimal sampled-data control systems*. Springer, London, ISBN: 3-540-19949-7.
- Clake, T., Ensor, J., & Griffin, S. J. (2003). Desirable eigenstructure for good short-term helicopter handling qualities: the attitude command response case. In *Proceedings of the institution of mechanical engineers part g - journal of aerospace engineering* (Vol. 217(1), p. 43-45).
- Clarke, T., & Griffin, S. J. (2004). An addendum to output feedback eigenstructure assignment: retro-assignment. *International Journal of Control*, 77(1), 78-85.
- Farineau, J. (1989). Lateral electric flight control laws of civil aircraft based on eigenstructure assignment technique. *AIAA Guidance Navigation and Control Conference*.
- Fletcher, L. (1981). On pole placement in linear multivariable systems with direct feedthrough i. theoretical considerations. *International Journal of Control*, 33(4), 729-749.
- Kimura, H. (1975). Pole assignment by gain output feedback. *IEEE Transactions on Automatic Control*, 20, 509-516.
- Kshatriya, N., Annakkage, U. D., Hughes, F. M., & Gole, A. M. (2007). Optimized partial eigenstructure assignment-based design of a combined pss and active damping controller for a DFIG. *Power Systems, IEEE Transactions on*, 25(2), 866–876.
- Liu, G. P., & Patton, R. J. (1998). *Eigenstructure assignment for control system design*. Wiley, Chichester.

- 1  
2  
3  
4  
5  
6  
7  
8  
9  
10  
11  
12  
13  
14  
15  
16  
17  
18  
19  
20  
21  
22  
23  
24  
25  
26  
27  
28  
29  
30  
31  
32  
33  
34  
35  
36  
37  
38  
39  
40  
41  
42  
43  
44  
45  
46  
47  
48  
49  
50  
51  
52  
53  
54  
55  
56  
57  
58  
59  
60
- Liu, Y., Tan, D. L., Wang, B., & Wang, X. (2013). Linear-matrix-inequality-based fault diagnosis for gas turbofan engine using eigenstructure assignment principle. *Applied Mechanics and Materials*, 302, 759–764.
- Moore, B. (1976). On the flexibility offered by state feedback in multivariable systems beyond closed loop eigenvalue assignment. *IEEE Transactions on Automatic Control*, 21, 689-692.
- Ouyang, H., Richiedei, D., Trevisani, A., & Zanardo, G. (2012). Discrete mass and stiffness modifications for the inverse eigenstructure assignment in vibrating systems: Theory and experimental validation. *International Journal of Mechanical Sciences*, 64(1), 211–220.
- Patton, R. J., Liu, G., & Patel, Y. (1995). Insensitivity properties of multi-rate feedback control systems. *IEEE Transactions on Automatic Control*, 40(2), 337-342.
- Piou, J., & Sobel, K. M. (1994). Yaw pointing and lateral translation using robust sampled data eigenstructure assignment. *Journal of Guidance, Control and Dynamics*, 17(5), 1133-1135.
- Piou, J., & Sobel, K. M. (1995). Robust multirate eigenstructure assignment with flight control application. *Journal of Guidance, Control and Dynamics*, 18(3), 539-546.
- Pomfret, A. J. (2006). *Eigenstructure assignment for helicopter flight control*. Unpublished doctoral dissertation, University of York.
- Pomfret, A. J., & Clarke, T. (2009). Desirable eigenstructure for good short-term helicopter handling qualities: the rate command response case. In *Proceedings of the institution of mechanical engineers part g - journal of aerospace engineering* (Vol. 223(G8), p. 1059-1065).
- Pomfret, A. J., Clarke, T., & Ensor, J. (2005). Eigenstructure assignment for semi-proper systems: pseudo-state feedback. In *IFAC world congress*.
- Roppenecker, G., & O'Reilly, J. (1989). Parametric output feedback controller design. *Automatica*, 25, 259-265.
- Sheng, J., Chen, T., & Shah, S. (2002). Generalized predictive control for non-uniformly sampled systems. *Journal of Process Control*, 12, 875-885.
- Shi, F., & Patton, R. J. (2012). Low eigenstructure sensitivity eigenstructure assignment to linear parameter varying systems. In *Ukacc* (p. 166-171).
- Sobel, K. M., Banda, S. S., & Yeh, H. (1989a). Robust control for linear systems with structured state space uncertainty. *International Journal of Control*, 50(5), 1991-2004.
- Sobel, K. M., Banda, S. S., & Yeh, H. (1989b). Structured state space robustness with connection to eigenstructure assignment. *American Control Conference*, 966-973.
- Sobel, K. M., & Lallman, F. (1989). Eigenstructure assignment for the control of highly augmented aircraft. *Journal of Guidance, Control, and Dynamics*, 12, 318-324.
- Srinathkumar, S. (1978). Eigenvalue/eigenvector assignment using output feedback. *IEEE Transactions on Automatic Control*, 23, 79-81.
- Tangirala, A., Li, D., Patwardhan, R., Shah, S., & Chen, T. (2001). Ripple-free conditions for lifted multirate control systems. *Automatica*, 37, 1637-1645.
- Wahrburg, A., & Adamy, J. (2013). Parametric design of robust fault isolation observers for linear non-square systems. *Systems and Control Letters*, 62(5), 420–429.
- White, B. A. (1995). Eigenstructure assignment: a survey. *Proceedings of the Institute of Mechanical Engineers*, 209, 1-11.
- White, B. A., Bruyere, L., & Tsourdos, A. (2007). Missile autopilot design using quasi-LPV polynomial eigenstructure assignment. *Aerospace and Electronic Systems, IEEE Transactions on*, 43(4), 1470-1483.
- Yu, W., Piou, J. E., & Sobel, K. M. (1993). Robust eigenstructure assignment for the extended medium range air to air missile. *Automatica*, 29(4), 889-898.
- Zhao, L., & Lam, J. (2016a). Dominant pole and eigenstructure assignment for positive systems with state feedback. *International Journal of Systems Science*, 47(12), 2901-2912.
- Zhao, L., & Lam, J. (2016b). Multiobjective controller synthesis via eigenstructure assignment with state feedback. *International Journal of Systems Science*, 47(13), 3219-3231.